Bull. Mater. Sci., Vol. 25, No. 3, June 2002, pp. 227–230. © Indian Academy of Sciences.

Transparent conducting zinc oxide thin film prepared by off-axis rf magnetron sputtering

M K JAYARAJ*, ALDRIN ANTONY and MANOJ RAMACHANDRAN
Department of Physics, Cochin University of Science and Technology, Kochi 682 022, India

MS received 18 December 2001; revised 29 April 2002

Abstract. Highly conducting and transparent ZnO : Al thin films were grown by off-axis rf magnetron sputtering on amorphous silica substrates without any post-deposition annealing. The electrical and optical properties of the films deposited at various substrate temperatures and target to substrate distances were investigated in detail. Optimized ZnO : Al films have conductivity of 2200 S cm^{-1} and average transmission in the visible range is higher than 85%. The conductivity and mobility show very little temperature dependence.

Keywords. Transparent conductors; ZnO thin films; photovoltaics.

1. Introduction

Zinc oxide is an *n*-type semiconductor with a wide direct band gap of 3·3 eV. Thin films of ZnO find application as transparent conducting electrode in photovoltaics, in place of expensive tin doped In_2O_3 (ITO) in displays (Addonizo *et al* 1999) and electric transducers (Yamamoto and Yoshida 1999). More recently, reports on possible *p*-type doping of ZnO have aroused much interest in ZnO thin films (Minegishi *et al* 1997; Joseph *et al* 1999; Yamamoto and Yoshida 1999; Ryu *et al* 2000).

Doping of ZnO films with Al, Ga, In, Ge has been reported to improve their electrical properties (Wang *et al* 1996). Al doped ZnO films have been widely studied and have low resistivity of $2–5 \times 10^{-4}$ Ωcm which is comparable to that of ITO films.

Several deposition techniques have been used to grow doped and undoped ZnO thin films including chemical vapour deposition (Hu and Gordan 1992), magnetron sputtering (Chang *et al* 2000), spray pyrolysis (Reddy *et al* 2000), pulsed laser deposition (Kim *et al* 2000), chemical beam deposition (Sato *et al* 1993) and evaporation (Ma Jin *et al* 1999).

Crystalline ZnO films with very smooth surface have been synthesized by off-axis sputtering (Zhu *et al* 2000). In this paper we report optimization of substrate temperature, gas pressure, substrate to target distances and orientation of the substrate with respect to the target in order to get highly conducting, transparent, smooth and crystalline films.

*Author for correspondence

2. Experimental

The ZnO films were prepared by rf magnetron sputtering in the off-axis sputtering geometry as shown in figure 1. The sputtering targets were prepared from the powder of ZnO (reagent grade 99 + %) and aluminum oxide with purity of 99·99 + %. In the case of Al doped samples, the ZnO and Al_2O_3 powders were mixed using agate mortar and pestle. The powder was pressed and sintered at 900°C for 10 h in air with a intermediate grinding. Two types of targets, one pure ZnO, and another with 2% of Al were used for the deposition of the films. Before depositing the films, the ZnO target surfaces were cleaned by pre-sputtering under the film deposition conditions for 30 min. The films were deposited at various substrate to target distances, substrate temperatures, rf power and sputtering pressures.

The sputtering was carried out in a pure Ar atmosphere. The resistivity of the ZnO and ZnO : Al films were found to increase drastically when oxygen was introduced together with the sputtering gas. In the preparation of transparent and conducting metal oxide thin films it is essential that non-stoichiometric metal rich oxide films be deposited (Chopra *et al* 1983). In the present study, amorphous silica was used as substrate for film deposition. The film growth temperature was measured by a thermocouple attached to substrate holder placed over the heater block.

The structure of thin films and targets was analysed using an X-ray diffractometer. Electron probe micro analysis (EPMA) was used to analyse the actual dopant concentration. Atomic force microscope (AFM) was used to study the film morphology. The conductivity and Hall coefficients were determined by four-point probe in van der Pauw configuration. Transmittance

was measured using a UV–vis–NIR spectrometer. The film thickness was measured using the interference method.

3. Results and discussion

The film growth conditions were optimized to have highly conducting transparent films. The film deposition was carried out in off-axis geometry as shown in figure 1. The off-axis configuration results in non-uniform film thickness across the substrate. The deposition rate is higher at the points on substrate that are near the target and it decreases as the points on the substrate move further away from the target. However, off-axis configuration gives much better results than on-axis configuration. To minimize the film non-uniformity, the quartz substrate of 1 × 1 cm was used for deposition and evaluation of electrical and optical properties. All the data presented here are for the films grown on amorphous silica substrates at a pressure of 10 m torr. The deposition rate was obtained as the ratio between the film thickness and the sputtering time. The thickness was determined by the optical interference method. The deposition rate is directly proportional to the rf power as shown in figure 2. Keeping the substrate to target height at 2·5 cm, the deposition rate was found to fall drastically as the substrate to target distance increased (figure 3). Beyond 2 cm substrate to target distance, the deposition rate is too low because the substrate is outside the plasma.

The conductivity of the ZnO : Al sputtered films increases with increasing substrate temperature and show a maximum around 423 K (figure 4) and falls very rapidly above the substrate temperature of 523 K. The composition analysis by EPMA shows that aluminum composition in the film is the same as that of the target and independent of the substrate temperature.

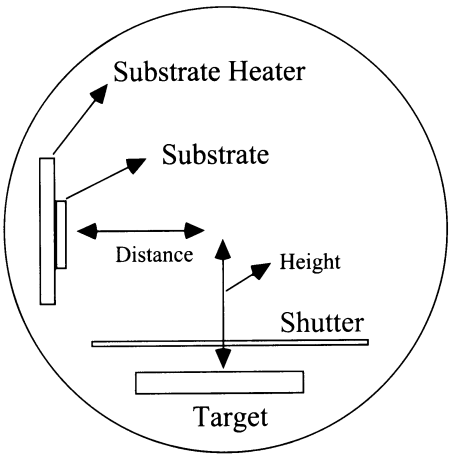

Figure 1. The off-axis sputtering configuration used for deposition of ZnO films.

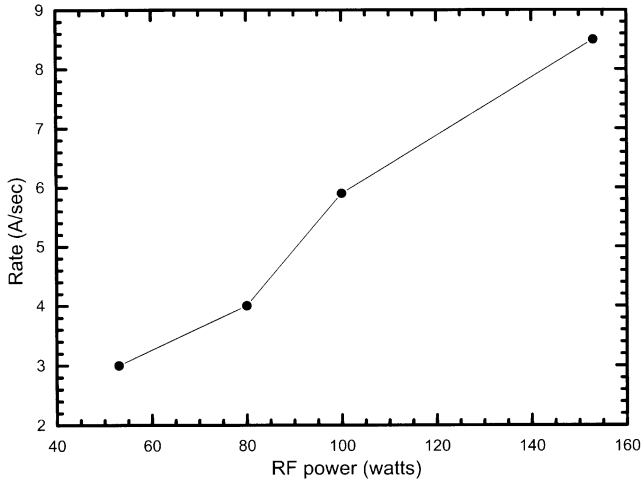

Figure 2. Variation of sputtering rate with rf power.

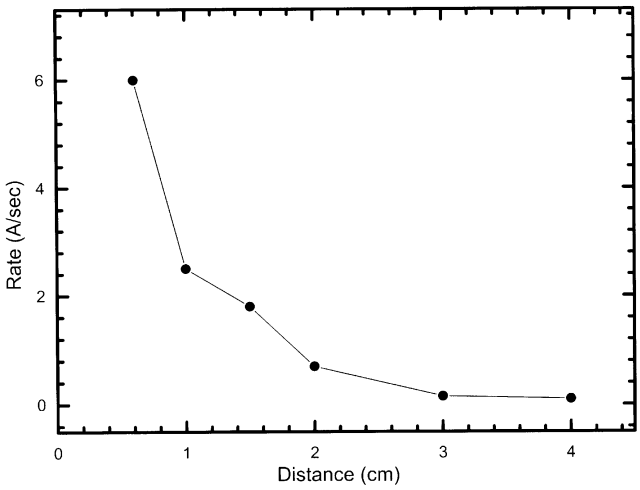

Figure 3. Variation of deposition rate with substrate to target distance.

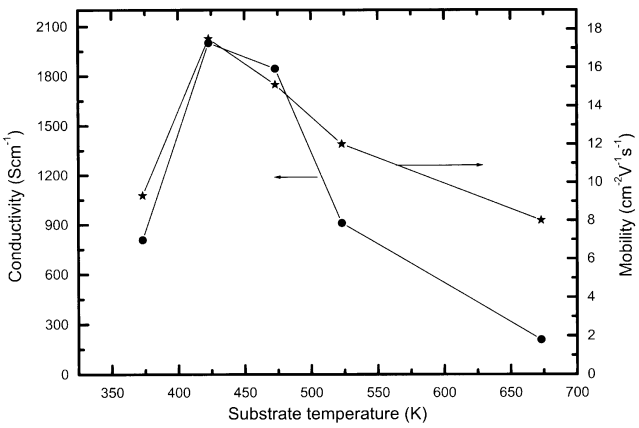

Figure 4. The conductivity and mobility of ZnO : Al films deposited at various substrate temperatures.

The AFM observation indicates that all the films are very smooth and have very similar morphology independent of the substrate temperature. The change in conductivity is due to both change in carrier concentration as well as the mobility as indicated by Hall measurements. The increase in carrier concentration may be due to the formation of metal rich oxide films. The best film properties in terms of conductivity and transmission were obtained for a substrate temperature of 423 K. Figure 5 shows the variation of conductivity and mobility as function of substrate to target distance, keeping the substrate to target height at 2·5 cm. Higher conductivity was observed for films deposited at the substrate to target distance of 1·5 cm. The Hall measurement shows that the higher conductivity is due to the increase in both carrier concentration as well as mobility of the carriers. The resistivity of both ZnO : Al and ZnO films show very little dependence on temperature (figure 6). It can be observed that the resistivity of undoped ZnO increases slightly with decreasing temperature. This dependence is too small in the case of ZnO : Al films. The nearly temperature independence of the resistivity confirms that the Al doped ZnO films are degenerate semiconductors.

The X-ray diffraction patterns of the ZnO films and the targets are shown in figure 7. The X-ray diffraction shows only 002 and 004 peaks indicating the strong preferred orientation; the *c* axis of the grains are uniformly perpendicular to the substrate surface. The surface energy density of the 002 orientation is the lowest in a ZnO crystal (Chopra *et al* 1983). Grains with lower surface energy will become larger as the film grows. Then the growth orientation develops into one crystallographic direction of the lowest surface energy. This means that 002 texture of the film may easily form. ZnO : Al films are highly transparent and show > 85% transmission in the visible region irrespective of the

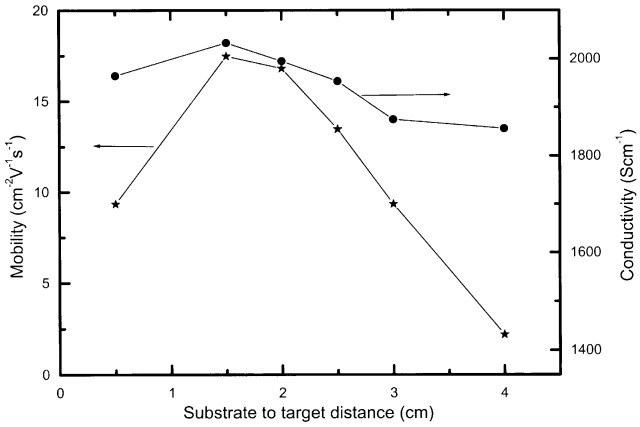

Figure 5. Conductivity and mobility of ZnO : Al films at various substrate to target distances (height 2·5 cm).

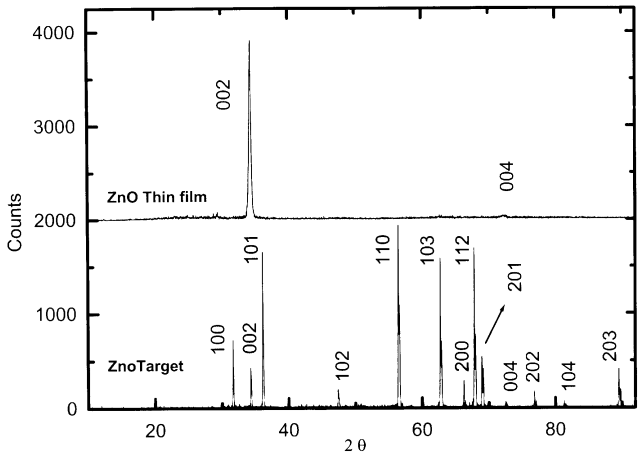

Figure 7. X-ray diffraction pattern of ZnO : Al target and ZnO : Al film grown on amorphous silicon substrate.

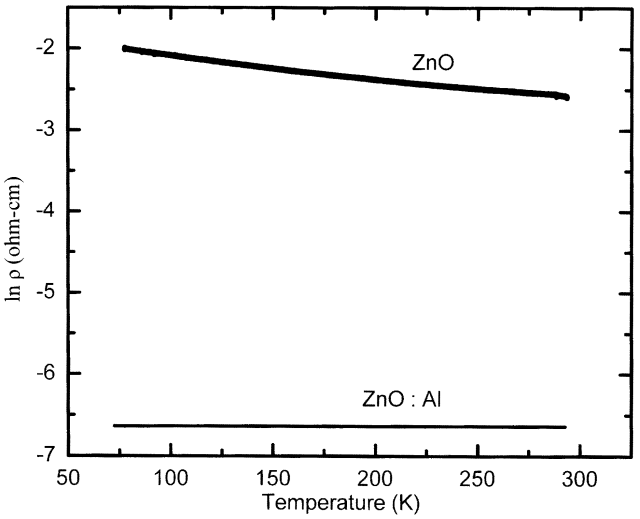

Figure 6. ln *r* resistivity vs temperature plot for ZnO : Al and ZnO films.

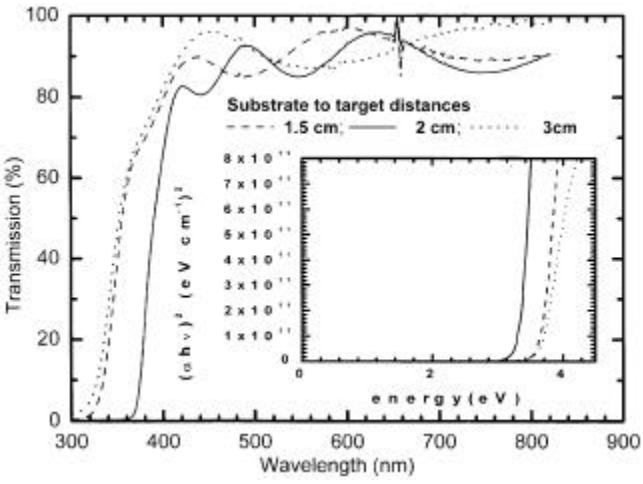

Figure 8. Transmission spectra of ZnO : Al films deposited at various substrate to target distances (height 2·5 cm). Inset shows the plot of $(ahn)^2$ vs *hn*.

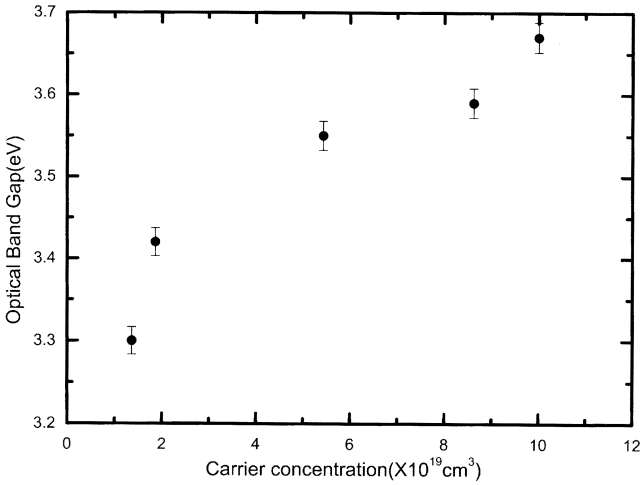

Figure 9. Variation of optical band gap of ZnO : Al film with carrier concentration.

doping as well as the substrate to target distance. The transmission spectrum of ZnO : Al films deposited under identical sputtering conditions but varying the substrate to target distance is given in figure 8. All the films exhibit a transmission of > 85% in the visible region. However, there is a shift in the absorption band edge. The shift in the absorption edge can be accounted for in terms of the increase in carrier concentration and blocking of low energy transitions which causes a Burstein Moss effect, which enhances the optical band gap. Figure 9 shows the variation of the optical band gap with electron density of ZnO : Al films. The carrier concentration was obtained from Hall measurement data and the optical band gap was evaluated from the transmission spectra. The absorption coefficient a was evaluated using the measured value of thickness 't' using the relation

$$I = I_0 e^{-at}.$$

The optical absorption coefficient 'a' near the absorption edge is given by

$$a \propto A (hn - E_{op})^{1/2} / hn.$$

The direct band gap of ZnO thin film was estimated by plotting $(\alpha\, hn)^2$ vs hn and extrapolating the linear portion near the onset of absorption edge to the energy axis. The optical band gap shows an increase with increasing carrier concentration. The optical gap is defined as the minimum energy needed to excite an electron from the valence band to the conduction band. In pure undoped crystals the optical gap equals the energy separation between the band edges. On heavy doping, the donor electrons occupy states at the bottom of the conduction band, since Pauli principle prevents states from being doubly occupied, the optical band gap is given by the energy difference between the states with Fermi momentum in the conduction and valence band. This type of blocking of low energy transitions is known as Burstein–Moss effect (Roth *et al* 1982; Sernelius *et al* 1988).

4. Conclusions

Undoped zinc oxide and aluminum doped zinc oxide films were prepared by rf magnetron sputtering of pre-synthesized target. All the films exhibit a transmission of over 85% in the visible region. The electrical resistivity of the film strongly depends on the substrate temperature, substrate to target distance and orientation of the substrate with respect to target. The increase in conductivity is due to the increase of carrier concentration and also due to the increased mobility of the carriers. Under the optimized deposition condition the ZnO : Al film shows a resistivity $4{\cdot}5 \times 10^{-4}$ ohm cm with transparency of > 85%. Morphology of the films shows that the films are very smooth.

Acknowledgements

The work was supported by the Department of Science and Technology, New Delhi, under SP/SM/M-63/96 and partially by AICTE.

References

Addonizo M L, Antonaia A, Cantele G and Privato C 1999 *Thin Solid Films* **349** 93

Chang J F, Wang H L and Hon M H 2000 *J. Cryst. Growth* **211** 93

Chopra K L, Major S and Pandaya D K 1983 *Thin Solid Films* **102** 1

Hu J and Gordan R G 1992 *J. Appl. Phys*. **72** 5381

Joseph M, Tabata H and Kawa T 1999 *Jpn J. Appl. Phys*. **A11** L1205

Kim H *et al* 2000 *Appl. Phys. Lett*. **76** 259

Ma Jin, Ji Feng, De-Heng Z, Ma Hong-Li and Li Shu-Ying 1999 *Thin Solid Films* **357** 98

Minegishi K, Kikuchi Y and Yano K 1997 *Jpn J. Appl. Phys*. **36** L1453

Reddy K T R, Gopalaswamy H, Reddy P J and Miles R W 2000 *J. Cryst. Growth* **210** 516

Roth A P, Webb J B and Williams D F 1982 *Phys. Rev*. **B25** 7836

Ryu Y R, Zhu S, Look D C, Wrobel J M, Amjeony and White H W 2000 *J. Cryst. Growth* **216** 330

Sato H, Minami T, Takata S, Miyata T and Ishii M 1993 *Thin Solid Films* **236** 14

Sernelius B E, Berggren K F, Jin Z C, Hamberg I and Granqvist C 1988 *Phys. Rev*. **B37** 10244

Wang R, King L H and Sleight A W 1996 *J. Mater. Res*. **11** 1659

Yamamoto T and Yoshida H 1999 *Jpn J. Appl. Phys*. **B2** L1453

Zhu S, Su C H, Lehouzky S L, Peters P and George M A 2000 *J. Cryst. Growth* **211** 106